Journal of Zhejiang University-SCIENCE A (Applied Physics & Engineering)
ISSN 1673-565X (Print); ISSN 1862-1775 (Online)
www.jzus.zju.edu.cn; www.springerlink.com
E-mail: jzus@zju.edu.cn

Independent volume-in and volume-out control of an open circuit pump-controlled asymmetric cylinder system*

Jing YAO†[1,2,3], Pei WANG[3], Xiao-ming CAO[3], Zhuo WANG[3]

[1]*The Laboratory of Heavy Machinery Fluid Power Transmission and Control in Hebei, Yanshan University, Qinhuangdao 066004, China*

[2]*National and Local Joint Engineering Center for Advanced Forging Press Forming Technology and Equipment Faculty of Engineering, Yanshan University, Qinhuangdao 066004, China*

[3]*Yanshan University, Qinhuangdao 066004, China*

†E-mail: jyao@ysu.edu.cn

Received Dec. 16, 2016; Revision accepted May 26, 2017; Crosschecked Jan. 31, 2018

Abstract: To avoid the flow asymmetry of a closed circuit pump-controlled asymmetric cylinder system, an efficient open circuit pump-controlled asymmetric cylinder system (OPACS) with an independent displacement volume-in and volume-out (VIVO) control method is proposed. The energy transmission path of the OPACS was analyzed, and an energy calculation model was built. A position-pressure combined control method was adopted to validate the proposed OPACS. Based on a 0.6-MN open circuit pump-controlled forging press system, a series of experiments with different return cylinder pressures were conducted. The experimental results confirmed that the proposed OPACS with the position-pressure combined control method was able to recover energy to reduce the installment power without sensitivity to the return cylinder's pressure variation and that the position accuracy and rapidity could be improved by increasing the pressure in the return cylinder.

Key words: Pump-controlled system; Asymmetric cylinder; Energy dissipation; Position-pressure combined control; Independent volume-in and volume-out (VIVO) control

https://doi.org/10.1631/jzus.A1600780 **CLC number:** TH137.7

1 Introduction

With growing concerns over energy shortage and environmental issues, the use of energy-saving hydraulic systems is becoming more urgent than ever. Thus, pump-controlled hydraulic systems have been attracting more attention in recent years due to their high transmission efficiency, simple structure, and low cooling power (Quan, 2008; Chiang, 2011).

Pump-controlled hydraulic systems have been investigated for decades and have been widely applied in engineering machinery, including vibration rollers, cement mixers, and asphalt pavers (Rose and Ivantysynova, 2011). Generally, pump-controlled hydraulic cylinder systems can be divided into two categories: a pump-controlled symmetrical cylinder system, such as a ship's rudder (Su and Jiang, 2010), and a pump-controlled asymmetric cylinder system, such as wheel-loaders, injection molding machines, and skid-steer loaders (Imamura et al., 2008; Peng et al., 2014). The pump-controlled symmetrical cylinder system has been extensively studied because of its flow control performance and high transmission efficiency. The idea that a hydraulic symmetrical linear cylinder could be driven directly combined with a direct-drive electric actuator has been proposed (Habibi and Goldenberg, 2000). An electric motor-pump compound control aircraft actuator system was

* Project supported by the National Natural Science Foundation of China (No. 51575471) and the Key Project of Natural Science Foundation of Hebei Province (No. E2016203264), China

ORCID: Jing YAO, https://orcid.org/0000-0002-0696-4754

analyzed in order to improve the reverse relationship between its efficiency and rapidity (Sha and Li, 2004), improving its overall performance. Asymmetric cylinders play a crucial role in engineering due to their large carrying capacity, simple structure, and low cost. As a result, a half closed circuit pump-controlled asymmetrical cylinder system (HCPACS) was proposed, as shown in Fig. 1. The Maha Fluid Power Research Center, Germany has investigated an HCPACS, utilizing displacement control (DC) to control multi-actuator motion and optimize its power management (Zimmerman and Ivantysynova, 2010; Hippalgaonkar and Ivantysynova, 2016a, 2016b), and it has been implemented in off-highway machines and excavators. This technology has demonstrated energy-savings, reductions in cooling power requirements, and improvements in control (Busquets and Ivantysynova, 2015a, 2015b). Additionally, another application of the HCPACS–direct drive volume control fuel injection system greatly improves the control of ship speed (Zheng et al., 2010; Sanada and Miyazaki, 2016). However, flow asymmetry characteristics of the differential cylinder (Quan and Lian, 2005; Ge et al., 2015), which lead to poor control and increased energy losses (Zhao et al., 2013; Wang et al., 2016), are still a big challenge for HCPACS. Several control methods such as the discrete-time sliding mode control method (Liu and Söffker, 2007) and a combination of robust nonlinear control and the feedback linearization method (Cho and Helduser, 2008) have been designed and investigated, and have improved control characteristics. An additional problem facing closed circuit pump-controlled asymmetrical cylinder system (CPACS) is cavitation damage. To prevent this damage, the fluid is delivered into the circuit by an anti-cavitation valve. Furthermore, CPACS require a charge pump for leakage and flushing, which leads to increased energy consumption.

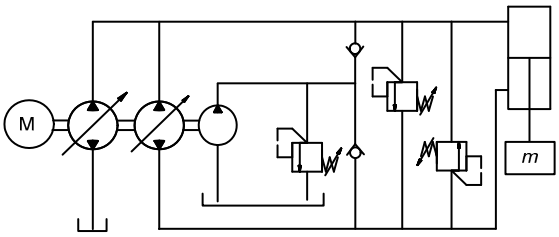

Fig. 1 Schematic diagram of the HCPACS (*m* is the mass of load)

To address the above issues, a novel open circuit pump-controlled asymmetric cylinder system (OPACS) is proposed, and a position-pressure combined control strategy, based on independent volume-in and volume-out (VIVO) control, is designed. In this study, the energy consumption characteristics and system control features of the proposed system are experimentally evaluated.

2 OPACS configuration

This study takes a fast-forging press utilizing an OPACS as the applied subject. The OPACS schematic is depicted in Fig. 2, where the key components are two bi-directional variable displacement pumps 1 and 2, each with different displacements, supplied by the Moog Company, USA. The pumps connect the rodless cavity and the rod cavity of the asymmetric differential cylinder 5, respectively, and the relief valve 6 is used to limit the maximum safety pressure of this system. The gear pump 3 is used to supply flow to pilot servo valves of the bi-directional variable displacement pumps 1 and 2, and the maximum control pressure depends on the relief valve 7. The coaxial bi-directional variable displacement pumps 1 and 2 and gear pump 3 connect with the electric motor 4 mechanically. Thus, the system employs triple-link pumps, which reduces installation space and cost.

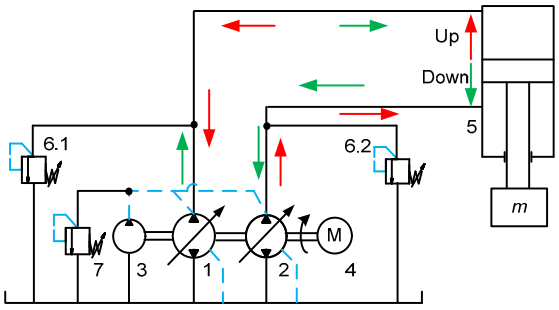

Fig. 2 Schematic diagram of the OPACS

Regardless of whether the asymmetric cylinder 5 is in the down-stroke or up-stroke position, one bi-directional variable pump is in a pumping condition and takes oil from the reservoir and delivers fluid into the asymmetric cylinder, while the other bi-directional variable pump is in the motor condition as

an actuator that recovers the hydraulic energy from the asymmetric cylinder.

In OPACS, the flow rate pumped to the cylinder chamber or delivered to the bi-directional variable pump can be controlled independently by adjusting the displacement of the corresponding bi-directional variable pump. We call this structure an independent displacement VIVO control system.

Compared with the HCPACS shown in Fig. 1, the main distinguishing factor is that an OPACS pumps the total flow from the reservoir, while the return oil from the cylinder is not fed back to the pump. Additionally, in the OPACS, because of the independent displacement VIVO configuration, there are no anti-cavitation valves or low pressure and large flow filling systems required. The OPACS not only reduces the cooling power but also enhances energy efficiency.

Of further importance is that the independent displacement VIVO system removes the inlet and outlet load coupling of a variable displacement pump and supplies more control freedom than the HCPACS, and so contributes to increased precision of control and to energy efficiency. Moreover, the OPACS not only supplies energy from the pump as it is consumed by the cylinder but also recovers energy from an assistant load, which decreases the installed power.

3 Energy transmission model

The energy conversion process of the OPACS is shown in Fig. 3. The electric motor gets active power P from the power grid. Then, one bi-directional variable pump converts mechanical energy P_4 into hydraulic energy (P_{11}, P_{21}), another bi-directional variable pump working as a motor recovers energy (P_{22}, P_{12}) from the actuator. The hydraulic energy (P_{11}, P_{21}) is used to overcome the total load power P_L, which consists of the external load force, friction, inertia force, and back-pressure. The gear pump constantly functions as an energy dissipation device and supplies power to control the variable displacement pumps 1 and 2 (pump 1 and pump 2 for short).

When the asymmetric cylinder is in the down-stroke, the bi-directional variable displacement pumps 1 and 2 are in the pump condition and motor condition, respectively. The output power (P_{11}) of pump 1 and the recovered power (P_{22}) of pump 2 can be described as

$$P_{11}=\frac{p_{p1}\cdot D_{p1}\cdot n\cdot \eta_1}{60}\times 10^{-6}, \tag{1}$$

$$P_{22}=\frac{p_{m2}\cdot D_{m2}\cdot n}{60}\times 10^{-6}, \tag{2}$$

where p_{p1} is the pump 1 outlet pressure in the pump condition, p_{m2} is the pump 2 inlet pressure in the motor condition, D_{p1} and D_{m2} are the displacements of pumps 1 and 2 in the pump and motor conditions, respectively, n is the speed of the co-axial electric motor and pumps, and η_1 is the volume efficiency of pump 1.

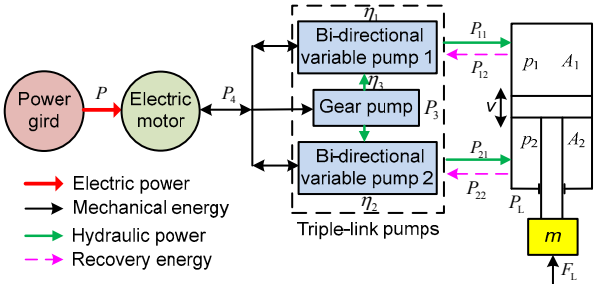

Fig. 3 Energy flow diagram of the OPACS (F_L is the force of total load; other variables are explained in the text)

Similarly, in the up-stroke stage, the bi-directional variable displacement pump 1 is in the motor condition, whereas pump 2 is also in the pump condition. The recovered power (P_{12}) of pump 1 and the output power (P_{21}) of pump 2 can be respectively described as

$$P_{12}=\frac{p_{m1}\cdot D_{m1}\cdot n}{60}\times 10^{-6}, \tag{3}$$

$$P_{21}=\frac{p_{p2}\cdot D_{p2}\cdot n\cdot \eta_2}{60}\times 10^{-6}, \tag{4}$$

where p_{m1} is the pump 1 outlet pressure in the motor condition, p_{p2} is the pump 2 inlet pressure in the pump condition, D_{m1} and D_{p2} are the displacements of pumps 1 and 2 in the motor and pump conditions, respectively, and η_2 is the pump 2 volume efficiency.

The gear pump input power (P_3) can be described as

$$P_3 = \frac{p_3 \cdot D_3 \cdot n \cdot \eta_3}{60} \times 10^{-6}, \quad (5)$$

where p_3 is the gear pump outlet pressure, D_3 is the displacement of the gear pump, and η_3 is the volume efficiency of the gear pump.

For the cylinder, the total input power is equal to the output power in the down-stroke stage and up-stroke stage, shown respectively in Eqs. (6) and (7):

$$P_{11} / \eta_1 - P_{22}\eta_2 = (p_1 A_1 - p_2 A_2)v = P_L, \quad (6)$$

$$P_{21} / \eta_2 - P_{12}\eta_1 = (p_2 A_2 - p_1 A_1)v = P_L, \quad (7)$$

where p_1 and p_2 are the pressures of the rodless cavity and rod cavity, A_1 and A_2 are the areas of the rodless cavity and rod cavity, respectively, v is the load velocity, and P_L is the consumed power of the total load.

In a working cycle, the electric motor receives the active energy E, and the energy transmission efficiency is η. The gear pump energy consumption E_3 is a constant. According to the energy conservation law and neglecting pipeline losses, the relationship between the output power of the electric motor and the total consumption power can be described as

$$E_4 = E \cdot \eta = E_{11} + E_{21} - E_{12} - E_{22} + E_3 = E_L, \quad (8)$$

where

$$E_{11} = \int_0^t \frac{P_{11}}{\eta_1} \mathrm{d}t, \ E_{12} = \int_0^t \frac{P_{12}}{\eta_1} \mathrm{d}t,$$

$$E_{21} = \int_0^t P_{21}\eta_2 \mathrm{d}t, \ E_{22} = \int_0^t P_{22}\eta_2 \mathrm{d}t,$$

$$E_3 = \int_0^t \frac{P_3}{\eta_3} \mathrm{d}t, \ E_L = \int_0^t P_L \mathrm{d}t.$$

From Eq. (8), the output energy of the electric motor E_4 is used by gear pump E_3, pump 1 E_{11}, and pump 2 E_{21}. Concurrently, the output energy of the electric motor E_4 is reduced due to the variable displacement pumps 1 and 2 working in the motor condition; the recovered energy (E_{21}, E_{22}) contributes to a decrease in the installation power of the OPACS.

This paper takes a traditional and typical position control fast-forging hydraulic system as an example; the fast-forging velocity variation is almost the same in the down-stroke stage and the up-stroke stage. Generally, accumulators are connected directly with the rod-cavity to stabilize its pressure and to improve the speed of a traditional fast-forging hydraulic system. From Eq. (8), if the rod-cavity pressure p_2 remains unchanged, then the recovered energy E_{22} approximately equals the consumed energy E_{21}. Therefore, the value of the pressure in the rod cavity has a little effect on the input power of the OPACS on the premise that p_2 remains unchanged. From the perspective of energy-saving and control accuracy, the rodless cavity adopts closed-loop position control and achieves position accuracy; meanwhile the rod cavity pressure closed-loop control is designed to validate the finding discussed above. The position-pressure combined method control chart is shown in Fig. 4. Moreover, to determine how this pressure variation in the rod cavity influences the control characteristics, further experimental research must be completed with different pressures in the rod cavity.

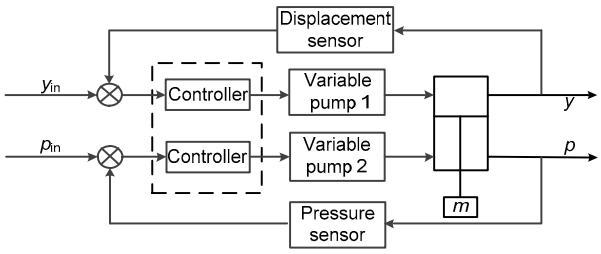

Fig. 4 Position-pressure combined control for the OPACS
y_{in}: signal of displacement; y: actual displacement; p_{in}: signal of pressure; p: actual pressure

4 Test platform

To evaluate the characteristics of the proposed OPACS, experiments on its control performance and energy consumption were conducted on a 0.6-MN fast-forging system in our laboratory, as shown in Fig. 5. The press system consists of two parts: a press body with a displacement sensor (Fig. 5a) and a hydraulic system (Fig. 5b). The maximum output force of the forging capacity is 0.6 MN. The body utilizes a pre-stressed structure with three beams and four pillars. The main specifications of the press are listed in Table 1.

High-response bi-directional servo variable displacement pumps in series (Fig. 5b) from the Moog Company were used to support the OPACS. A coaxial

gear pump connected with a variable displacement pump supplies control fluid to the pilot valves of the variable displacement pumps.

An xPC-Target Data control & acquisition system with a 1-ms sample time was used in the electrical control system. The position-pressure combined control strategy based on MATLAB/Simulink was programmed and downloaded to xPC-Target. xPC-Target then controlled the servo variable pumps by ACL6126 (D/A conversion). The displacement and pressure signals were collected by PCL1716 (A/D conversion). Interface software was developed using Labview to accomplish the key parameters real-time set and display the values of the press.

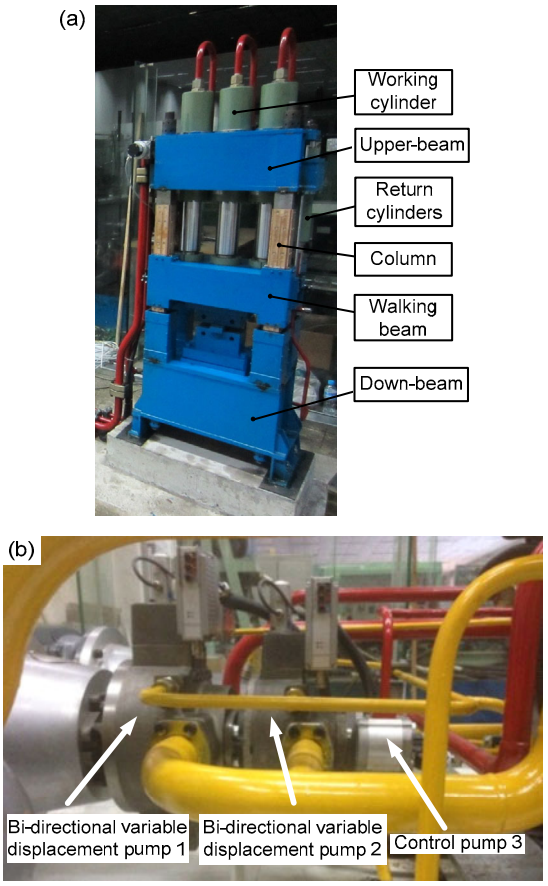

Fig. 5 Test bench of the open circuit hydraulic pump-controlled forging press system
(a) 0.6-MN fast-forging system; (b) Moog triple-link pumps

5 Results and discussion

According to previous experiments and investigation, the pressure in the return cylinders was set about 9 MPa and could overcome external load force, friction, inertia force, back-pressure, etc. If the pressure in the return cylinders has a lower value, it would take a long time to reach system pressure and have bad effect on rapidity. Therefore, in order to evaluate how the different return cylinder pressure values influence the position control and energy consumption, in the following experiments, a sinusoid with a 1 Hz forging frequency and a 10 mm amplitude was set for the position control system. The return cylinder pressures were set as 9 MPa, 12 MPa, and 15 MPa. In the experiments, blocks of lead were used to simulate load variation of the heated forging work piece. The length, breadth, and height of the forging workpiece were 300 mm, 40 mm, and 40 mm, respectively.

5.1 Control characteristics analysis

The displacement of the working cylinder, the pressure in the return cylinder, and the pressure in the working cylinder using the new control strategy are shown in Fig. 6.

Table 1 Hydraulic system parameters of 0.6-MN forging press

Parameter	Value	Note
Working cylinder diameter (m)	0.1	
Return cylinder diameter (m)	0.045	
Bi-directional variable pump 1 displacement (ml/r)	80	50 ms to 80 ms
Bi-directional variable pump 2 displacement (ml/r)	45	50 ms to 80 ms
Gear pump displacement (ml/r)	8	
Electric motor power (kW)	30	
Electric motor torque (N·m)	191	
Pressure transmitter (MPa)	0–40	±0.1%
Displacement sensor (mm)	700	16-bit accuracy

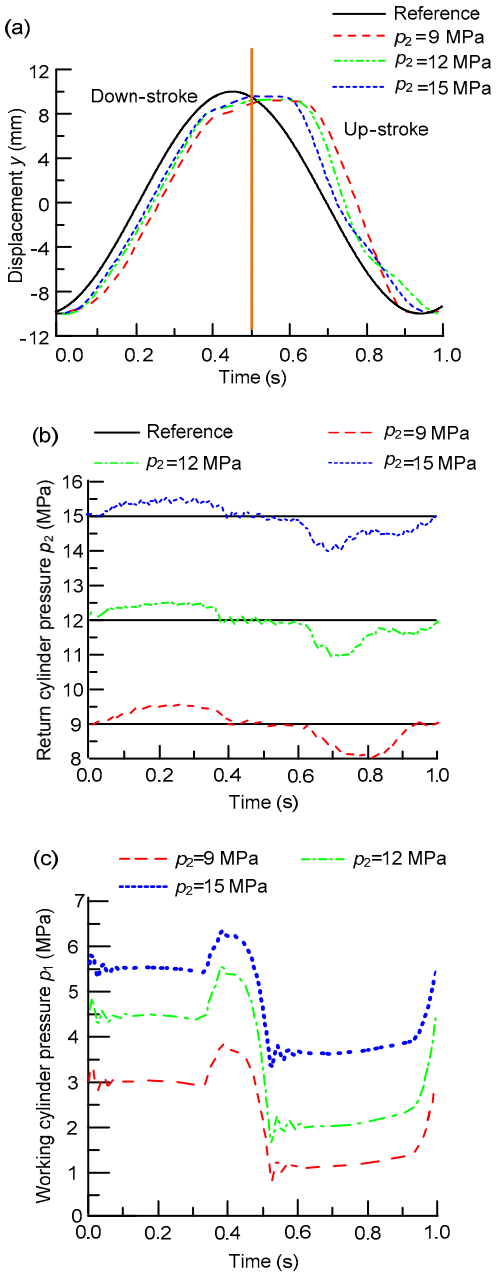

Fig. 6 Comparison of the position of the pressure in the return cylinder and the working cylinder with different back-pressures

(a) Working cylinder displacement response curve; (b) Return cylinder pressure curve; (c) Working cylinder pressure curve

In Fig. 6a, it can be seen that increasing the pressure p_2 in the return cylinder from 9 MPa to 12 MPa and ultimately to 15 MPa decreased the position error (the difference between the input setting y_{in} and the real displacement y in the down-stroke stage) from 0.8 mm to 0.4 mm. Additionally, the maximum phase lag was approximately 0.08 s, which indicated not only that the press successfully tracked the required forging input but also that the higher pressure in the return cylinder resulted in higher precision and faster response.

From Fig. 6b, by using closed-loop pressure control, the maximum pressure error of the return cylinder was limited to 0.5 MPa in the down-stroke stage and 1 MPa in the up-stroke stage. Fig. 6c shows that the pressure in the working cylinder increases with an increase in the return cylinder pressure. Higher back-pressure in the return cylinder results in a higher load on the working cylinder.

5.2 Energy analysis

Eqs. (1)–(4) can be used to calculate the power of the two bi-directional variable displacement pumps under different return cylinder pressures in one working cycle, as shown in Fig. 7. When the power has a positive value, the pump supplies power to the system. When the power has a negative value, it recovers energy from the system.

Fig. 7 shows that in the down-stroke stage, with the return cylinder's pressure p_2 increasing from 9 MPa to 12 MPa and ultimately to 15 MPa, the variable pump 1 needs to supply more power to overcome the back-pressure load, and thus, the output power of pump 1 grows. While pump 2 is in the motor condition, more power is supplied and more power is recovered by pump 2. In the up-stoke stage, pump 1 is in the motor condition, while the pump 2 is in the pump condition. When the back-pressure increases, both increase.

Based on Eqs. (1)–(8) and considering a single forging cycle, the electric motor output energy, the total consumption energy including the variable pumps and the gear pump, and the total recovered energy in the motor condition were calculated, as shown in Fig. 8. It can be seen that with an increase in pressure in the return cylinder p_2, the pump consumption energy and the recovered energy increased. However, the electric motor output energy remained nearly unchanged, with 1268 J, 1271 J, and 1272 J corresponding to the return cylinder pressure p_2= 9 MPa, 12 MPa, and 15 MPa, respectively. Therefore, the pressure in the return cylinder has little effect on the open circuit pump-controlled forging press hydraulic system.

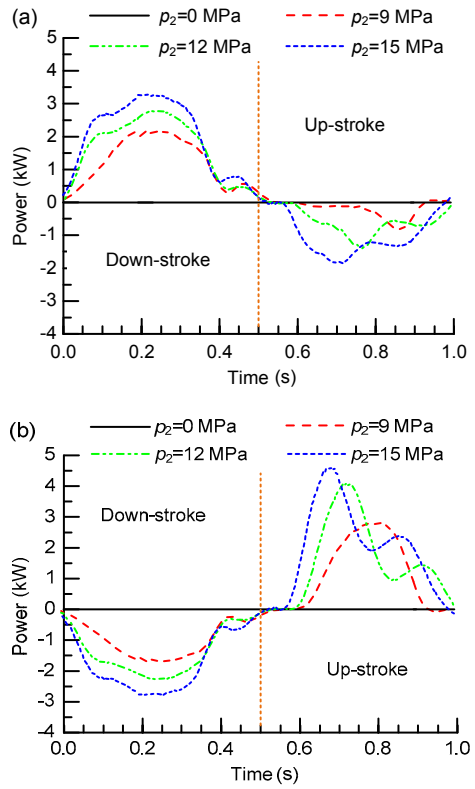

Fig. 7 Power comparison of pump 1 and pump 2 with different back-pressures

(a) Output power of variable pump 1; (b) Output power of variable pump 2

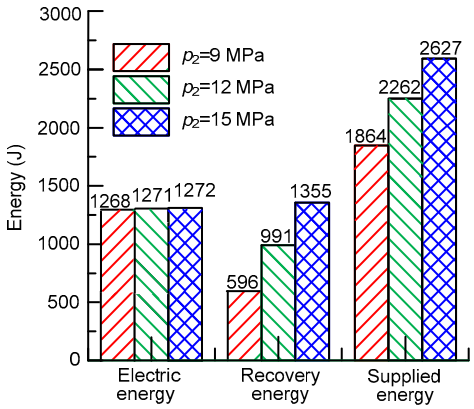

Fig. 8 Energy distribution comparison with different back-pressures

6 Conclusions

With respect to energy saving in pump-controlled systems, a more efficient OPACS has been proposed to improve the control freedom and realize energy recovery. To validate the control characteristics and energy consumption of the proposed OPACS, a position-pressure combined control method was adopted. Based on a 0.6-MN forging press, a series of experiments were conducted, and the test results confirmed that the OPACS control accuracy and rapidity improved by increasing the pressure in the return cylinder. However, the electronic input power of the OPACS changed little, indicating that the OPACS is effective at reducing the installed power as well as improving control characteristics.

Despite the fact that the independent VIVO control method of the OPACS shows great potential in control characteristics and energy savings, some challenges, including parameter coupling between the position control system and the pressure control system, as well as the high cost of variable pumps compared to valve-controlled systems, will be investigated in future research.

References

Busquets E, Ivantysynova M, 2015a. A multi-actuator displacement-controlled system with pump switching: a study of the architecture and actuator-level control. *Transactions of the Japanese Fluid Power System Society*, 8(2):66-75.

Busquets E, Ivantysynova M, 2015b. Adaptive robust motion control of an excavator hydraulic hybrid swing drive. *SAE International Journal of Commercial Vehicles*, 8(2):568-582. https://doi.org/10.4271/2015-01-2853

Chiang MH, 2011. A novel pitch control system for a wind turbine driven by a variable-speed pump-controlled hydraulic servo system. *Mechatronics*, 21(4):753-761. https://doi.org/10.1016/j.mechatronics.2011.01.003

Cho SH, Helduser S, 2008. Robust motion control of a clamp-cylinder for energy-saving injection moulding machines. *Journal of Mechanical Science and Technology*, 22(12):2445-2453. https://doi.org/10.1007/s12206-008-0907-6

Ge L, Dong Z, Huang W, et al., 2015. Research on the performance of hydraulic excavator with pump and valve combined separate meter in and meter out circuits. IEEE International Conference on Fluid Power and Mechatronics, p.37-41.

Habibi S, Goldenberg A, 2000. Design of a new high-performance electro hydraulic actuator. *IEEE/ASME Transactions on Mechatronics*, 5(2):158-164. https://doi.org/10.1109/3516.847089

Hippalgaonkar R, Ivantysynova M, 2016a. Optimal power management for DC hydraulic hybrid multi-actuator machines—Part 1: Theoretical studies, modeling and

simulation. *Journal of Dynamic Systems, Measurement, and Control*, 138(5):051002. https://doi.org/10.1115/1.4032742

Hippalgaonkar R, Ivantysynova M, 2016b. Optimal power management for DC hydraulic hybrid multi-actuator machines—Part 2: Machine implementation and measurement. *Journal of Dynamic Systems, Measurement, and Control*, 138(5):051003. https://doi.org/10.1115/1.4032743

Imamura T, Sawada Y, Ichikawa M, 2008. Energy-saving hybrid hydraulic system comprising highly efficient IPM motor and inverter, for injection molding and manufacturing machine. Proceedings of the JFPS International Symposium on Fluid Power, p.117-120.

Liu Y, Söffker D, 2007. Robust approach for position control of hydraulic differential cylinder. Proceedings of the ASME International Design Engineering Technical Conferences & Computers and Information in Engineering Conference, p.27-32.

Peng Y, Wang J, Wei W, 2014. Model predictive control of servo motor driven constant pump hydraulic system in injection molding process based on neurodynamic optimization. *Journal of Zhejiang University-SCIENCE C (Computers & Electronics)*, 15(2):139-146. https://doi.org/10.1631/jzus.C1300182

Quan L, 2008. Current state, problems and the innovative solution of electro-hydraulic technology of pump controlled cylinder. *Chinese Journal of Mechanical Engineering*, 44(11):87-92 (in Chinese). https://doi.org/10.3901/JME.2008.11.087

Quan L, Lian ZS, 2005. Improving the efficiency of pump controlled differential cylinder system with inlet and outlet separately controlled principle. *Chinese Journal of Mechanical Engineering*, 41(3):123-127 (in Chinese). https://doi.org/10.3901/JME.2005.03.123

Rose J, Ivantysynova M, 2011. A study of pump control systems for smart pumps. Proceedings of the 52nd National Conference on Fluid Power, p.683-692.

Sanada K, Miyazaki T, 2016. Application of DDVC fuel injection system to ship speed control. BATH/ASME Symposium on Fluid Power and Motion Control, No. FPMC2016-1760. https://doi.org/10.1115/FPMC2016-1760

Sha N, Li J, 2004. Research on airborne power-by-wire integrated electrical actuation and control system. *Journal of Beijing University of Aeronautics and Astronautics*, 30(9): 909-912 (in Chinese).

Su WH, Jiang JH, 2010. Direct drive volume control electro-hydraulic servo ship rudder. *Key Engineering Materials*, 439-440:1388-1392. https://doi.org/10.4028/www.scientific.net/KEM.439-440.1388

Wang X, Tao JF, Zhang FR, 2016. Precision position control of pump-controlled asymmetric cylinder. *Journal of Zhejiang University (Engineering Science)*, 50(4):597-602 (in Chinese). https://doi.org/10.3785/j.issn.1008-973X.2016.04.001

Zhao H, Zhang HJ, Quan L, 2013. Characteristics of asymmetrical pump controlled differential cylinder speed servo system. *Journal of Mechanical Engineering*, 49(22): 170-176 (in Chinese). https://doi.org/10.3901/JME.2013.22.170

Zheng JM, Zhao SD, Wei SG, 2010. Fuzzy iterative learning control of electro-hydraulic servo system for SRM direct-drive volume control hydraulic press. *Journal of Central South University of Technology*, 17(2):316-322. https://doi.org/10.1007/s11771-010-0048-9

Zimmerman J, Ivantysynova M, 2010. Reduction of engine and cooling power by displacement control. Proceedings of the 6th FPNI PhD Symposium, p.339-352.

中文概要

题　目： 开式泵控非对称缸负载容腔独立控制系统

目　的： 为减少能量排放和提升节能效果，并解决非对称缸系统的流量不对称问题，本文对开式泵控非对称缸负载容腔独立控制系统的控制特性及能耗特性进行了深入的研究，以期为其实际应用提供理论支撑。

创新点： 1. 提出开式泵控非对称缸负载容腔独立控制系统，建立其能量传输模型；2. 以压机为对象进行实验研究，采用位置压力负载容腔独立控制方法，获得其能耗与控制特性。

方　法： 1. 介绍开式泵控非对称缸负载容腔独立控制系统的构型；2. 通过理论推导，建立能量传输模型，得到具有能量回收功能的系统；3. 通过实验研究和分析，验证所提系统和方法的有效性。

结　论： 1. 基于能量传输模型得到的系统具有较好的节能特性；2. 开式泵控非对称缸负载容腔独立控制系统增加了系统控制自由度，验证了负载容腔独立控制方法的有效性；3. 开式泵控非对称缸负载容腔独立控制系统采用无杆腔位置控制和有杆腔压力控制组合的控制方法；随着有杆腔压力的提高，在不增加系统能耗的前提下该方法改善了系统的位置控制精度。

关键词： 泵控系统；非对称缸；能耗；位置压力组合控制；负载容腔独立控制